JCI The Journal of Clinical Investigation

# Interaction of mature CD3$^+$CD4$^+$ T cells with dendritic cells triggers the development of tertiary lymphoid structures in the thyroid

Tatjana Marinkovic, Alexandre Garin, Yoshifumi Yokota, Yang-Xin Fu, Nancy H. Ruddle, Glaucia C. Furtado, Sergio A. Lira

*J Clin Invest.* 2006;116(10):2622-2632. https://doi.org/10.1172/JCI28993.

**Research Article** **Immunology**

Ectopic expression of CC chemokine ligand 21 (CCL21) in the thyroid leads to development of lymphoid structures that resemble those observed in Hashimoto thyroiditis. Deletion of the *inhibitor of differentiation 2* (*Id2*) gene, essential for generation of CD3$^-$CD4$^+$ lymphoid tissue–inducer (LTi) cells and development of secondary lymphoid organs, did not affect formation of tertiary lymphoid structures. Rather, mature CD3$^+$CD4$^+$ T cells were critical for the development of tertiary lymphoid structures. The initial stages of this process involved interaction of CD3$^+$CD4$^+$ T cells with DCs, the appearance of peripheral-node addressin–positive (PNAd$^+$) vessels, and production of chemokines that recruit lymphocytes and DCs. These findings indicate that the formation of tertiary lymphoid structures does not require Id2-dependent conventional LTis but depends on a program initiated by mature CD3$^+$CD4$^+$ T cells.



# Interaction of mature CD3+CD4+ T cells with dendritic cells triggers the development of tertiary lymphoid structures in the thyroid

Tatjana Marinkovic,[1] Alexandre Garin,[1] Yoshifumi Yokota,[2] Yang-Xin Fu,[3] Nancy H. Ruddle,[4] Glaucia C. Furtado,[1] and Sergio A. Lira[1]

[1]Immunobiology Center, Mount Sinai School of Medicine, New York, New York, USA. [2]Department of Molecular Genetics, School of Medicine, University of Fukui, Fukui, Japan. [3]Department of Pathology, University of Chicago, Chicago, Illinois, USA. [4]Section of Immunobiology, Yale University School of Medicine, New Haven, Connecticut, USA.

**Ectopic expression of CC chemokine ligand 21 (CCL21) in the thyroid leads to development of lymphoid structures that resemble those observed in Hashimoto thyroiditis. Deletion of the *inhibitor of differentiation 2* (*Id2*) gene, essential for generation of CD3$^-$CD4$^+$ lymphoid tissue–inducer (LTi) cells and development of secondary lymphoid organs, did not affect formation of tertiary lymphoid structures. Rather, mature CD3$^+$CD4$^+$ T cells were critical for the development of tertiary lymphoid structures. The initial stages of this process involved interaction of CD3$^+$CD4$^+$ T cells with DCs, the appearance of peripheral-node addressin–positive (PNAd$^+$) vessels, and production of chemokines that recruit lymphocytes and DCs. These findings indicate that the formation of tertiary lymphoid structures does not require Id2-dependent conventional LTis but depends on a program initiated by mature CD3$^+$CD4$^+$ T cells.**

## Introduction

Secondary lymphoid structures, such as lymph nodes and Peyer patches, are formed during intrauterine life (1, 2). Lymphoid organogenesis depends on lymphoid tissue–inducer (LTi) cells with a characteristic CD3$^-$CD4$^+$CD45$^+$ phenotype (reviewed in refs. 1, 2). LTi cells also express lymphotoxin α1 β2 (LTα1β2), IL-7 receptor α (IL-7Rα), CC chemokine receptor 7 (CCR7), and CXC chemokine receptor 5 (CXCR5) (1). The development of LTi cells depends on the function of nuclear retinoid orphan receptor γ (RORγ), inhibitor of differentiation 2 (Id2), and TNF-related activation-induced cytokine (TRANCE); genetic inactivation of these molecules severely affects organogenesis of secondary lymphoid organs (3–5).

LTi cells exert their activity through interaction with stromal organizer cells. Molecular mediators of these interactions include LTα1β2 expressed by LTi cells and lymphotoxin β receptor (LTβR) expressed on the surface of stromal cells (1, 6). LTβR-deficient mice lack all lymph nodes, Peyer patches, and colon-associated lymphoid tissues (7). Similarly, treatment of female mice during pregnancy with an LTβR-fusion protein prevents formation of the lymph nodes and Peyer patches in the progeny (8). Interestingly, however, the phenotype of mice deficient for LTβ is somewhat different than that of the LTβR knockout mice; in the absence of LTβ, mesenteric, sacral, and cervical lymph nodes are still formed (9–12). This discrepancy suggests that other LTβR ligands may be important during lymphoid organogenesis. LIGHT is one such ligand (13). LIGHT deficiency does not affect normal lymphoid development, but when combined with LTβ deficiency, it impairs development of mesenteric lymph nodes (13).

The recruitment and retention of lymphocytes into lymphoid organ anlage requires the expression of adhesion molecules and chemokines (1, 6). Recruitment of lymphocytes into adult LN depends on the expression of homeostatic chemokines, such as CC chemokine ligand 21 (CCL21) (SLC), CCL19 (ELC), CXC chemokine ligand 13 (CXCL13) (BLC), and CXCL12 (SDF-1), on the surface of specialized vascular structures known as high endothelial venules (HEVs) (reviewed in ref. 14). In addition, the endothelial cells of HEVs express highly glycosylated and sulfated sialomucins, such as peripheral-node addressin (PNAd) (15), which interact with L-selectin expressed on naive lymphocytes and are required for lymphocyte trafficking in lymphoid organs. The cellular and molecular mechanisms responsible for HEV formation are not fully understood. The lymphotoxin (LT) ligand-receptor interaction appears to be important for differentiation of endothelial cells into HEVs (16, 17). In the absence of LTα or LTβ, expression of PNAd in nasal-associated lymphoid tissue (NALT) HEVs is strongly suppressed (17). LTα1β2 regulates HEV-restricted sulfotransferase (HEC-6ST), a key enzyme required to synthesize PNAd (18). Recent evidence supports a role for LTβR not only in the induction of HEV formation but also HEV homeostatic maintenance in lymphoid tissues (19).

Despite considerable progress in understanding secondary lymph node organogenesis, little is known about the mechanisms underlying the formation of tertiary lymphoid structures detected in chronic inflammatory diseases. Tertiary lymph node structure and cellular composition resemble that of secondary lymphoid organs, with segregated T and B cell zones and the presence of HEVs (20). Importantly, the lymph node–like organization correlates with the expression of homeostatic chemokines CCL21, CCL19, and CXCL13 (20, 21). In agreement with these observations, ectopic expression of CCL21, CCL19, and CXCL13 induces formation of the lymphoid structures in different organs (22–26). However, the precise mechanisms underlying these processes are unclear. In particular, it is unclear whether the formation of tertiary lymphoid structures requires conventional LTi cells. The intradermal injec-

**Nonstandard abbreviations used:** CCL21, CC chemokine ligand 21; CCR7, CC chemokine receptor 7; CXCL13, CXC chemokine ligand 13; CXCR5, CXC chemokine receptor 5; HEC-6ST, HEV-restricted sulfotransferase; HEV, high endothelial venule; Id2, inhibitor of differentiation 2; LT, lymphotoxin; LTα1β2, lymphotoxin α1 β2; LTi, lymphoid tissue–inducer (cell); LTβR, lymphotoxin β receptor; PNAd, peripheral-node addressin.

**Conflict of interest:** The authors have declared that no conflict of interest exists.

**Citation for this article:** *J. Clin. Invest.* **116**:2622–2632 (2006). doi:10.1172/JCI28993.

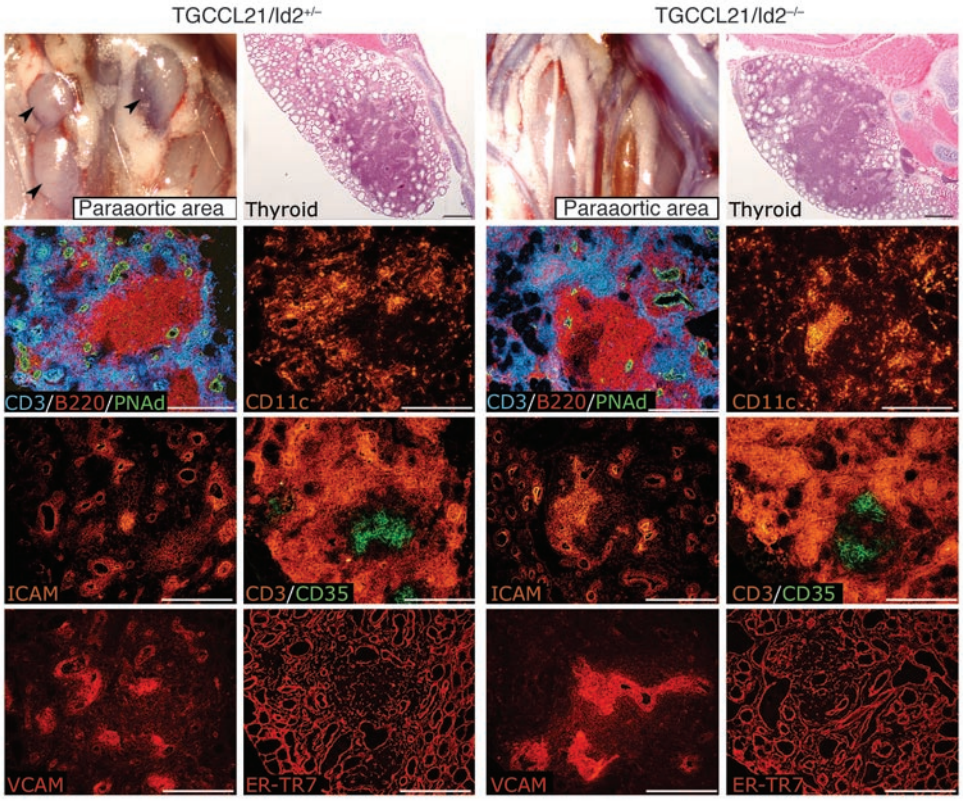


**Figure 1**
CCL21-induced formation of lymphoid structures in the thyroid does not depend on the activity of LTi cells. TGCC6/21 mice were crossed with *Id2*-deficient mice to obtain mice with thyroid-specific expression of chemokine and no LTi cells (referred to as TGCCL21/Id2$^{-/-}$ mice). Lymph nodes were present in TGCCL21/Id2$^{+/-}$ (arrowheads) and absent in TGCCL21/Id2$^{-/-}$ mice ($n = 4$). All TGCL21/Id2$^{-/-}$ mice analyzed had lymphocytic infiltrates in the thyroid that were morphologically indistinguishable from the ones observed in TGCCL21/Id2$^{+/-}$ mice. Note segregation of B (B220$^+$) and T (CD3$^+$) cells, the presence of PNAd$^+$ HEVs, upregulation of ICAM and VCAM expression, accumulation of CD11c$^+$ DCs, clusters of CD35$^+$ follicular DCs, and the presence of an ER-TR7$^+$ reticulum meshwork in both strains. Scale bars: 0.25 mm.

tion of newborn mesenteric lymph node–derived cells (containing stromal organizer cells and LTi cells but not mature lymphocytes) into an adult mouse induces the formation of lymphoid structures in the skin (27). This study convincingly demonstrates the ability of LTi to induce the formation of lymphoid structures but does not clarify whether LTi cells are required for the formation of tertiary lymphoid structures that occur in adult life.

Here we show that the formation of tertiary lymphoid structures in the thyroid is promoted by mature CD3$^+$CD4$^+$ T cells and not by canonical LTi cells. We also show that mature CD3$^+$CD4$^+$ T cells promote development of PNAd$^+$ vessels in the thyroid via a CCR7- and LTβR-dependent mechanism.

## Results

*CCL21-induced formation of lymphoid structures in the thyroid does not depend on the activity of LTi cells.* The importance of LTi cells for the formation of secondary lymphoid organs has been well documented (1). *Id2*-deficient mice that lack LTi cells fail to develop lymph nodes and Peyer patches (4, 28). However, it has been unclear whether LTis are required for the development of tertiary lymphoid structures in adults. Recently, we have shown that transgenic expression of CCL21 in the thyroid induces formation of tertiary lymphoid tissue (24). We used this model to test whether chemokine-driven lymphocytic infiltration of the thyroid requires LTi cells. We crossed TGCCL21 mice to *Id2*-deficient mice to obtain mice that lack LTi cells and express CCL21 in the thyroid (referred to as TGCCL21/Id2$^{-/-}$ mice). As expected, TGCCL21/Id2$^{-/-}$ mice did not develop lymph nodes or Peyer patches (Figure 1). However, the thyroids of TGCCL21/Id2$^{-/-}$ mice had lymphoid aggregates indistinguishable from those found in TGCCL21/Id2$^{+/-}$ mice (Figure 1). Within these aggregates, we observed segregation of T and B cells, CD11c$^+$ DCs, PNAd$^+$ HEVs, clusters of CD35$^+$ follicular DCs within B cell areas, and organization of an ER-TR7$^+$ reticulum meshwork (Figure 1). Expression of the adhesion molecules ICAM and VCAM was also evident within these infiltrates (Figure 1). In summary, our findings strongly suggest that formation of tertiary lymphoid structures induced by expression of CCL21 in the thyroid does not depend on Id2-dependent conventional LTi cells.

*Kinetics of lymphocyte entry into the thyroid.* We have previously shown that adoptively transferred splenocytes infiltrate the thyroids of transgenic RAG mice expressing CCL21 (RAGTGCCL21 mice) but not the thyroids of RAG mice (24). To examine the mechanisms underlying the recruitment of splenocytes into the CCL21-expressing thyroids, we performed an additional series of adoptive transfers using cells isolated from GFP-transgenic mice (29). We examined the kinetics of cell accumulation in the thyroid 1, 3, and 5 days after cell transfer. To this end, we examined more than 80 sections derived from 4 mice at each time point. Very few GFP$^+$ cells were found within the thyroid on day 1 (1 cell/section in 20% of all sections examined) or day 3 (1–3 cells/section in 40% of the sections examined), but their number significantly increased on day 5 (>100 cells/section) (Figure 2A). In agreement with our previous data, immediate entry of the cells into the thyroid was not dependent on the expression of vascular addressins (24). Importantly, in all cases examined, large numbers of GFP$^+$ cells were found within lymph nodes even at day 1 (Figure 2A). These results suggest that most splenocytes first traffic into lymph nodes and that only a small number of them enter the thyroid despite high levels of expression of the chemokine CCL21 (not shown). The dramatic increase in the number of splenocytes in the thyroid between days 3 and 5 is thus likely due to cellular influx and proliferation.

To start examining the mechanisms responsible for entry/retention of lymphocytes into the thyroid, we focused on the role of CCR7. We have previously demonstrated a requirement for the

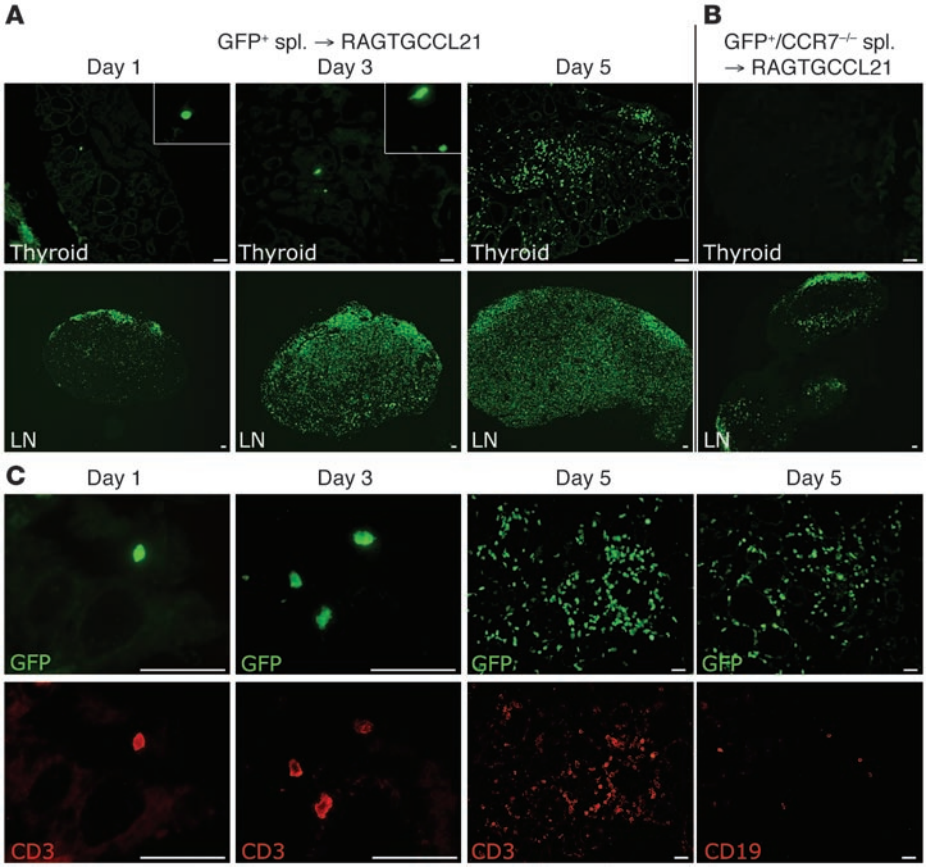


**Figure 2**
Kinetics of CCL21-driven entry of splenocytes (spl.) into the thyroid. GFP+ splenocytes ($10^7$) were injected into RAGTGCCL21 mice. At the indicated time points, thyroids and lymph nodes were analyzed for the presence of GFP+ cells. (**A**) Few GFP+ cells were found on days 1 and 3 (insets), but their number increased on day 5. Results shown are representative of 80 thyroid sections obtained from 4 mice at each time point. Magnification, ×40 (insets). (**B**) Splenocytes ($10^7$) from GFP-transgenic mice deficient for *CCR7* (GFP+/CCR7−/−) were injected into RAGTGCCL21 mice. Ten days later, thyroids and lymph nodes of the recipient mice were extensively analyzed (more than 20 sections/thyroid) for the presence of GFP+ cells. Shown are representative sections ($n$ = 3 mice). (**C**) All GFP+ cells present on days 1 and 3 in thyroids of RAGTGCCL21 mice stained with anti-CD3 antibody ($n$ = 4 mice in each group). Most GFP+ cells on day 5 are CD3+; however, at this time point, few CD19+ B cells could also be detected ($n$ = 4 mice). Scale bars: 0.05 mm.

chemokine receptor CCR7 in this process (24) but did not define whether CCR7 mediates this effect at the level of lymphocytes or other cells. To this end, we injected *CCR7*$^{+/+}$ and *CCR7*$^{-/-}$ GFP+ splenocytes into RAGTGCCL21 mice and examined their lymph nodes and thyroids 10 days later. As expected, mice injected with *CCR7*$^{+/+}$ cells had thyroid infiltrates. Mice injected with *CCR7*$^{-/-}$ cells had no thyroid infiltrates but had abnormally distributed GFP+ cells in lymph nodes, as previously described (30) (Figure 2B). These results suggest that expression of CCR7 in lymphocytes is required for the trafficking or retention of lymphocytes into the thyroid.

*The first cells that infiltrate the thyroid are CD3+ T cells.* To investigate the phenotype of the GFP+ cells that first infiltrate the thyroid, we analyzed thyroid sections stained with conventional antibodies against leukocyte surface molecules. All GFP+ cells present in thyroids on day 1 (0–1 GFP+ cell/section in $n$ = 4 mice) and day 3 (1–3 GFP+ cells/section in $n$ = 4 mice) were CD3+ (Figure 2C). CD3+ cells were the most prevalent cells in thyroids of RAGTGCCL21 mice at all time points analyzed (Figure 2C). In agreement with our previous findings (24), the vast majority of infiltrating cells were CD4+ (not shown). GFP+ B cells were not observed in thyroids on day 3 after transfer, but few were observed by day 5 (Figure 2C).

Next we purified CD4+ and CD8+ T cells and B220+ cells from spleens of GFP-transgenic mice and transferred them separately into RAGTGCCL21 mice. CD4+ T cells used in this and other experiments described here were CD3+CD4+ (Supplemental Figure 1; supplemental material available online with this article; doi:10.1172/JCI28993DS1). GFP+CD4+ T cells accumulated in RAGTGCCL21 thyroids with kinetics similar to those described for transfer of total splenocytes (Figure 3A), but sorted CD8+ T and B cells did not accumulate in thyroids of RAGTGCCL21 mice (Figure 3A). Both B220+ and CD8+GFP+ cells were, however, readily detected in the lymph nodes and spleens of recipient mice (Figure 3A). The finding that transferred B cells alone did not accumulate in thyroids of RAGTGCCL21 mice raised the possibility that B cell entry and/or survival in the tissue depended on factors induced by the entry of CD4+ T cells into the thyroid. To determine whether T cells facilitated entry of B cells into thyroids, we injected RAGTGCCL21 mice with GFP+CD3+CD4+ T cells and then 10 days later injected B cells purified from wild-type mice. Under these experimental conditions, large numbers of B cells infiltrated thyroids of RAGTGCCL21 mice 1 day after injection (Figure 3B). Taken together, the findings indicate that entry, retention, or survival of B cells in the thyroid is facilitated by previous infiltration of T cells.

*Incoming T cells cluster with host-derived DCs.* Next we determined whether the presence of GFP+CD3+CD4+ T cells in the thyroid would be associated with influx or redistribution of host-derived cells. The distribution of macrophages in thyroids of both RAG and RAGTGCCL21 mice was not changed by the presence of GFP+ T cells (not shown), but the distribution of DCs was significantly altered. Prior to injection, there were few homogeneously distributed host DCs in either RAG or RAGTGCCL21 thyroids (Supplemental Figure 2). In contrast, clusters of host DCs were observed around GFP+CD3+CD4+ T cells (Figure 4A). DC clustering correlated directly with the presence of GFP+ cells, and it was not observed in the absence of infiltrating cells. Clusters were observed as early as day 1 and were larger and more numerous by day 10 (Figure 4A). Most of the CD11c+ DCs

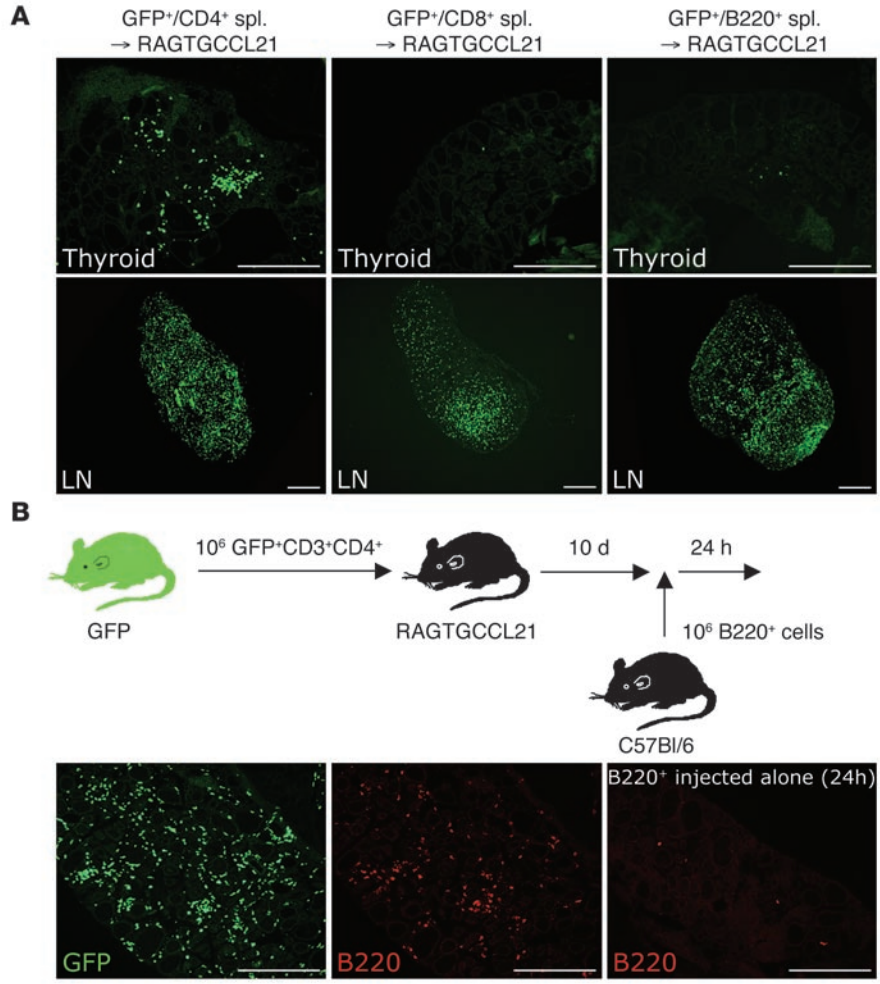


**Figure 3**
$CD3^+CD4^+$ T cells promote entry of B cells in the thyroid. (**A**) $CD4^+$ and $CD8^+$ T cells and $B220^+$ B cells were sorted from the spleen of GFP-transgenic mice and injected separately into RAGTGCCL21 mice for 5 days. While $CD3^+CD4^+GFP^+$ cells infiltrated the recipient thyroids in significant numbers, very few $B220^+$ or $CD3^+CD8^+$ T cells were found ($n$ = 4). In all cases, $GFP^+$ cells were readily detected in lymph nodes. (**B**) $GFP^+CD3^+CD4^+$ T cells ($1 \times 10^6$) were injected i.v. into RAGTGCCL21 mice. At day 10, mice were injected again with $B220^+$ cells purified from C57Bl/6 mice. As a control, RAGTGCCL21 mice were injected with $B220^+$ cells alone. Mice were sacrificed 24 hours later, and thyroids were examined for the presence of B cells. Shown are representative sections ($n$ = 3 mice). Scale bars: 0.25 mm.

were also $CD11b^+$ (data not shown). No DC/T cell clusters were ever observed in RAG thyroids after transfer of splenocytes ($n > 10$).

We also tested to determine whether adhesion molecules were expressed within the DC/T cell clusters. Overexpression of CCL21 in RAGTGCCL21 thyroids did not induce expression of ICAM and VCAM (not shown). However, intense ICAM and VCAM staining was observed in the vicinity of the infiltrating cells (Figure 4B). The expression of these adhesion molecules was restricted to the host cells (not $GFP^+$) (Figure 4B). Double staining revealed that host $CD11c^+$ DCs expressed both ICAM and VCAM (Figure 4B). In addition, the expression of these adhesion molecules was also evident on $CD11c^-$ host cells (Figure 4B). Upregulation of ICAM and VCAM expression in the areas of infiltration was also observed when *Id2*-deficient splenocytes were transferred into RAGTGCCL21 mice (Supplemental Figure 3). Expression of adhesion molecules in the absence of conventional LTi cells further argues in favor of the concept that mature T cells are sufficient to promote formation of lymphoid tissue in the thyroid.

To determine whether the increased number of DCs was due to their proliferation in situ, we transferred C57BL/6 splenocytes into RAGTGCCL21 mice for 5 days and stained thyroid sections using antibodies against Ki67, a cell proliferation marker. Many Ki67-positive cells were observed in thyroids of RAGTGCCL21 mice that had received splenocytes via adoptive transfer (Supplemental Figure 4). However, the vast majority of these cells were $CD3^+$ cells and not DCs (Supplemental Figure 4), suggesting that influx and not proliferation accounted for the increased number of DCs in the thyroids after adoptive transfer of lymphocytes. To determine whether $CD3^+CD4^+$ T cells promoted influx of DCs in the thyroid, we monitored the accumulation of GFP-labeled DCs in thyroids of RAGTGCCL21 mice. We injected RAGTGCCL21 mice with $CD3^+CD4^+$ T cells and then 5 days later injected $10^6$ $CD11c^+$ cells sorted from the bone marrow of $GFP^+$/Flt3 ligand–transgenic mice (31). Five days later, thyroids were analyzed for the presence of $GFP^+$ DCs. As a control, $GFP^+$ DCs were injected alone into RAG and RAGTGCCL21 mice. Comparable numbers of $GFP^+$ cells were present in the lymph nodes of all analyzed animals (Figure 4C). Very few $GFP^+$ DCs were present in the thyroids of RAGTGCCL21 mice injected with $GFP^+$ DCs alone (0–1 cell/section, 50 sections from each of 2 mice) (Figure 4C). However, $GFP^+$ DCs readily accumulated in the thyroids of RAGTGCCL21 mice previously injected with $CD3^+CD4^+$ T cells (8–10 cells/section, 40 sections from each of 2 mice) (Figure 4C). These findings indicate that $CD3^+CD4^+$ T cells facilitate entry of DCs in the thyroid.

To further understand the molecular mechanisms by which T cells attract other cell types into the thyroid, we compared the gene expression pattern of all known chemokines in thyroids of RAG and RAGTGCCL21 mice before and after transfer of $CD3^+CD4^+$ T cells (Figure 5). The injection of $CD3^+CD4^+$ T cells did not affect the expression profile of the chemokines in thyroids of RAG mice (Figure 5). With the

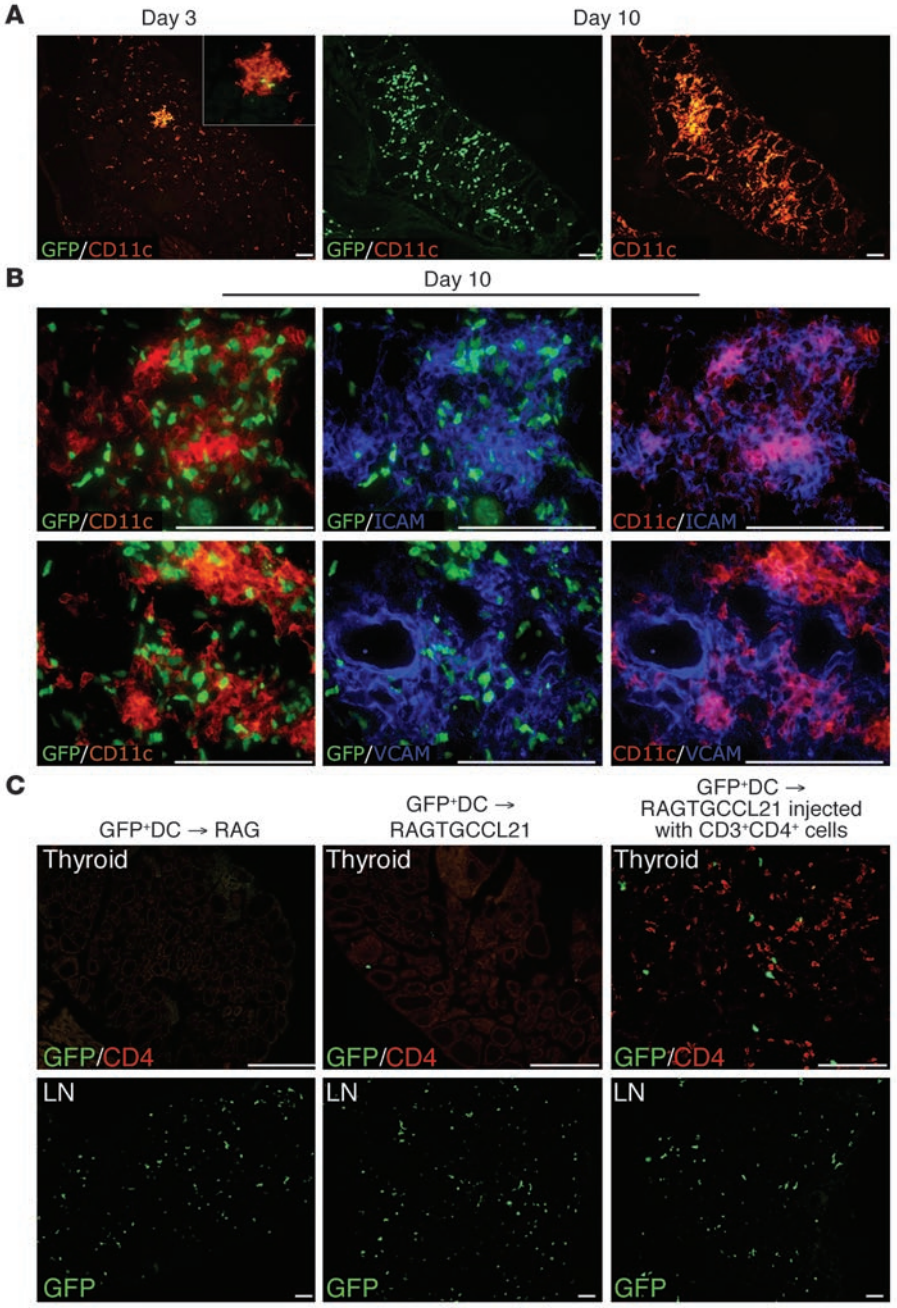


**Figure 4**
$CD3^+CD4^+$ T cell infiltration induces clustering of DCs and expression of adhesion molecules in the thyroid. $GFP^+CD3^+CD4^+$ T cells ($10^6$) were injected i.v. into RAGTGCCL21 mice. (**A**) Thyroids from mice sacrificed on days 3 and 10 were stained with anti-CD11c antibody for visualization of DCs. Inset shows higher magnification (×40) of the DC/T cell cluster present on day 3 after T cell transfer. (**B**) Double staining for CD11c (red) with ICAM (blue) or VCAM (blue) on day 10 revealed that adhesion molecules were expressed by DCs (magenta). Notice expression of VCAM on vessel cells as well as on host $CD11c^-$ cells. Shown are representative sections ($n = 3$ mice at each time point). (**C**) $CD3^+CD4^+$ T cells ($1 \times 10^6$) were injected i.v. into RAGTGCCL21 mice. At day 5, mice were injected again with $1 \times 10^6$ $CD11c^+$ cells sorted from the bone marrow of mice double transgenic for Flt3 ligand and GFP. As a control, $GFP^+$ DCs alone were injected into RAG and RAGTGCCL21 mice. After 5 days, thyroids of recipient mice ($n = 2$ in each group) were analyzed for the presence of $GFP^+$ cells. Representative sections are presented. Scale bars: 0.05 mm.

exception of CCL5, which was modestly upregulated (2-fold over RAG levels), the expression of chemokines was not upregulated in thyroids of RAGTGCCL21 mice (Figure 5), indicating that overexpression of CCL21 in the thyroid did not promote expression of other chemokines. However, the presence of infiltrating $CD3^+CD4^+$ T cells in thyroids of RAGTGCCL21 mice induced the expression of several inflammatory chemokines in the tissue (Figure 5). CXCL9, CXCL10, and CXCL11, chemoattractants for T cells, DCs, and activated B cells (32, 33), were the most upregulated chemokines. We also observed an increased expression of CXCL9, CXCL10, and CXCL11 mRNA in the cervical lymph nodes of transgenic mice after cell transfer (Supplemental Figure 5); however, the differences were much less pronounced than the differences observed in thyroids. The expression of CCL2, CCL5, CCL8, and CXCL16 was also increased in the thyroid, but not in lymph nodes (Supplemental Figure 5). CXCL12 and CXCL13, typical B cell chemoattractants (14, 34), were not significantly elevated by the presence of infiltrating $CD3^+CD4^+$ T cells 10 days after transfer. These results suggest that the interaction of incoming T cells with parenchymal cells stimulates the production of chemokines and adhesion molecules that promote the formation of a microenvironment suitable for further recruitment and retention of leukocyte subsets into the thyroid.

*DC influx and clustering are affected by CCR7 deficiency*. An important role for CCR7 in the migration of DCs into lymph nodes is well documented (30, 35). Therefore, we asked whether DC migration and clustering in the thyroid required CCR7 expression. We per-

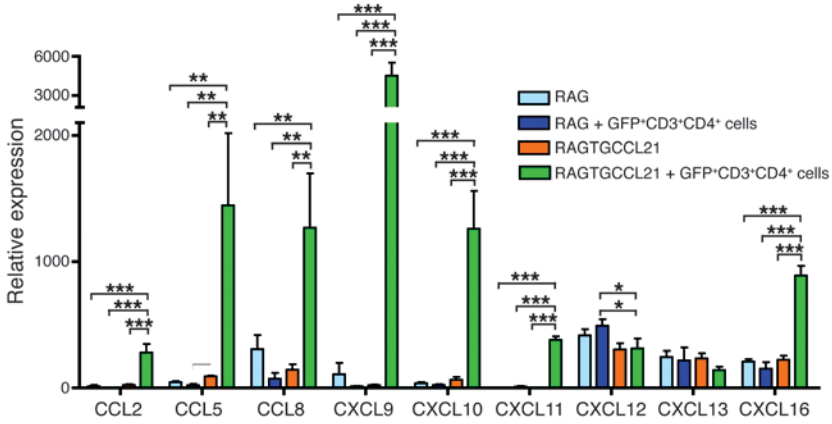


**Figure 5**
$CD3^+CD4^+$ T cell infiltration induces expression of chemokines. Total RNA was isolated from thyroids of RAG, RAGTGCCL21, and RAGTGCCL21 mice injected with $10^6$ $CD3^+CD4^+$ T cells for 10 days. The relative levels of mRNA of all known chemokines were determined by quantitative PCR performed in duplicate. Values shown are the mean ± SEM of $n = 3$ animals for each genotype. $^*P < 0.05$; $^{**}P < 0.01$; $^{***}P < 0.001$.

formed a series of crosses to obtain RAG mice that express CCL21 in the thyroid and lack CCR7 (RAGTGCCL21/$CCR7^{-/-}$ mice). CCR7 deficiency did not affect the number and distribution of DCs in thyroids prior to injection of lymphocytes (Supplemental Figure 2). *CCR7*-competent $GFP^+$ splenocytes transferred into *CCR7*-deficient RAGTGCCL21 hosts successfully infiltrated thyroids (Figure 6). Interestingly, *CCR7* deficiency on host cells affected clustering of DCs. DC clusters induced by the transfer of $GFP^+$ cells into RAGTGCCL21/$CCR7^{-/-}$ recipient mice were clearly reduced in number and in size compared with those of RAGTGCCL21/$CCR7^{+/+}$ recipients (Figure 6). Coincidently, the expression of CXCL9 and CXCL16, the chemokines that showed upregulation upon influx of T cells in the RAGTGCCL21 mice (Figure 5 and Figure 6B), was impaired in the CCR7-deficient recipients (Figure 6B). These findings suggest that expression of CCR7 on host cells is important for the migration or clustering of DCs in the thyroid upon influx of lymphocytes.

*Purified $CD4^+$ T cells induce formation of $PNAd^+$ vessels in the thyroid.* $PNAd^+$ vessels are important for lymphocyte trafficking into lymph nodes (15). $PNAd^+$ HEVs are found in secondary lymphoid organs and in nonlymphoid tissues during chronic inflammatory conditions or autoimmune diseases. However, the requirements for formation of $PNAd^+$ HEVs in nonlymphoid tissues are unknown. To identify the cell type responsible for the induction of PNAd expression, we looked for $PNAd^+$ vessels following transfer of defined cell subsets into RAGTGCCL21 mice. $PNAd^+$ vessels were first observed in thyroid samples 5 days after transfer of purified $CD3^+CD4^+$ T cells. By day 10, we detected $PNAd^+$ vessels in thyroids of all RAGTGCCL21 mice examined ($n > 50$ mice) (Figure 7A). No $PNAd^+$ vessels were present in thyroids of RAGTGCCL21 mice injected with $B220^+$ cells or in thyroids of RAG mice injected with $CD4^+$ T cells (not shown).

Interestingly, $PNAd^+$ vessels were always found in close proximity to the DC clusters (Figure 7A). To determine whether the interaction of DCs/T cells was required for the development of $PNAd^+$ vessels in the thyroid, we examined thyroids of RAGTGCCL21/$CCR7^{-/-}$ mice after transfer of $CD4^+$ T cells, as we have previously demonstrated a deficit in DC/T cell clustering in these animals (Figure 6). Under these conditions, no $PNAd^+$ structures were detected, even 1 month after transfer (Figure 7B). Therefore, we conclude that the DC/T cell interaction is a critical factor for the formation of $PNAd^+$ vessels in the thyroid.

*LTβR signaling regulates formation of PNAd structures in the thyroid.* Development of $PNAd^+$ HEVs in secondary lymphoid organs is dependent on LT/LTβR signaling (16–19). To determine whether LTβR plays a role in the formation of PNAd in the thyroid, we used a LTβR-IgG fusion protein that binds LTβR ligands (36, 37). RAGTGCCL21 mice were treated with the LTβR fusion protein or human IgG (LTβR-IgG) on days 1, 3, 5, and 7 after injection of purified $GFP^+CD4^+$ cells. LTβR-IgG treatment was not sufficient to disrupt already existing $PNAd^+$ HEVs in the lymph nodes (Figure 8A), affect lymphocyte entry in thyroids, or host DC clustering (Figure 8A and not shown) or ICAM and VCAM expression (Figure 8B). All mice from the control IgG-injected group developed $PNAd^+$ vessels in thyroids, but strikingly, none of the mice injected with the LTβR-IgG fusion protein had $PNAd^+$ vessels (>100 sections per thyroid, $n = 8$ mice) (Figure 8A). These findings suggest an important role for LTβR in the formation of $PNAd^+$ vessels in nonlymphoid tissue.

Interestingly, $PNAd^+$ vessels can be detected in thyroids of LTα-deficient TGCCL21 mice (ref. 24 and Figure 8C). To examine the contribution of LTα in the formation of HEVs in the thyroid, we examined the expression of HEC-6ST (38, 39). $PNAd^+$ vessels present in the TGCCL21 mice had high endothelium and expressed HEC-6ST, suggesting that these vessels were bona fide mature HEVs. In contrast, the endothelium of $PNAd^+$ vessels present in TGCCL21/$LT\alpha^{-/-}$ mice was flat and negative for HEC-6ST, resembling the residual flat venules that retain abluminal PNAd expression present in the mesenteric lymph nodes of $LT\beta^{-/-}$ mice, described by Drayton and colleagues (18) (Figure 8). Therefore, we conclude that, while abluminal expression of PNAd can be triggered in thyroids of TGCCL21 mice in the absence of LT, full maturation of these venules to HEVs during formation of tertiary lymphoid organs depends on LTα activity.

## Discussion

The formation of lymphoid structures in nonlymphoid tissues is a hallmark of autoimmune inflammatory diseases such as rheumatoid arthritis and Hashimoto thyroiditis. Transgenic expression of the chemokine CCL21, which is expressed in the thyroids of patients with autoimmune thyroiditis (40), leads to the formation of lymphoid structures in the thyroid (24), indicating a critical role for this molecule in the formation of tertiary lymphoid aggregates. Lymphoid structures observed in thyroids of TGCCL21 mice are indistinguishable from tertiary lymphoid tissue, as they contain segregated T and B lymphocytes, large numbers of DCs, organized follicular dendritic cell clusters, and specialized vascular structures. Our results indicate that formation of these lymphoid structures does not depend on conventional LTi cells as they develop in mice that lack Id2, a transcription regulator that is critical for differentiation of conventional LTi cells (4, 28). This finding raised the possibility that a cell different from

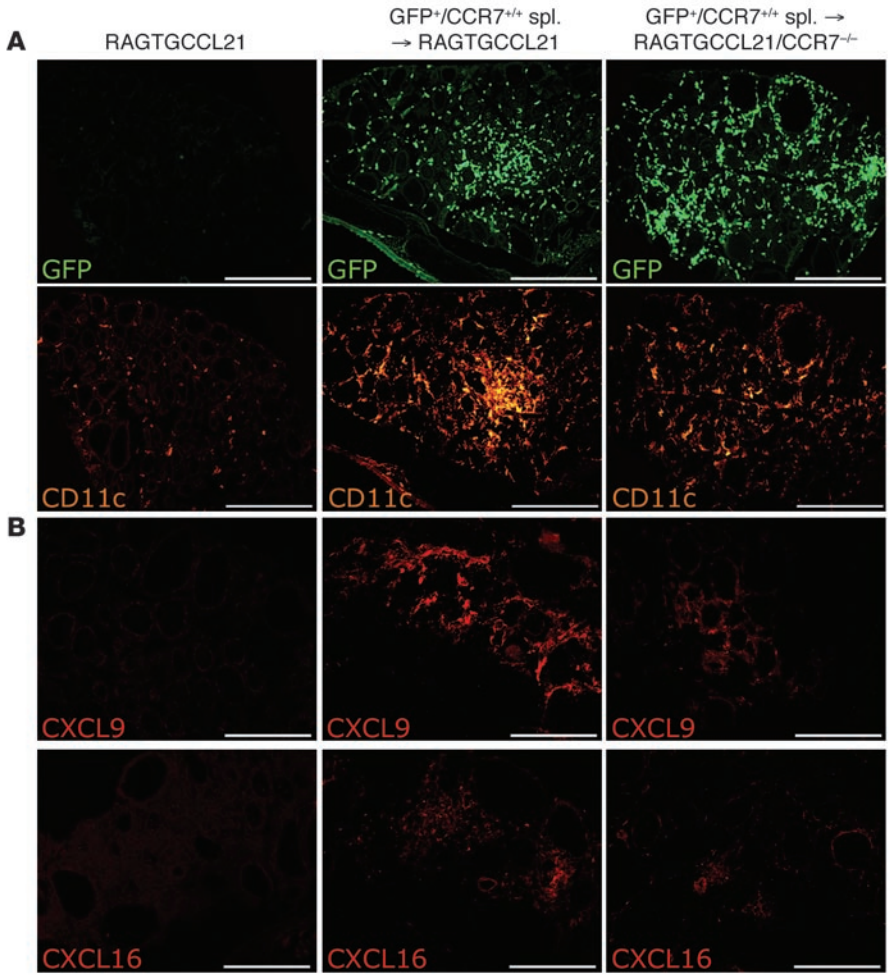


**Figure 6**
CCR7 is required for the formation of infiltrates. GFP$^+$ splenocytes ($10^7$) were transferred into RAGTGCCL21 mice deficient for *CCR7* (RAGTGCCL21/CCR7$^{-/-}$). (**A**) Although CCR7 deficiency of the host did not prevent entry of lymphocytes into thyroids, the CD11c$^+$ DC (yellow) clusters observed were small and less frequent. (**B**) Expression of CXCL9 and CXCL16, chemokines highly upregulated upon entry of T cells in thyroids of RAGTGCCL21 mice, was also impaired in the CCR7-deficient host. Shown are representative sections ($n$ = 4 mice). Scale bars: 0.25 mm.

conventional LTis initiated formation of tertiary lymphoid structures. The present study addresses the nature of this cell and the mechanisms involved in the formation of tertiary lymphoid structures. We show that chemokine-driven formation of lymphoid structures in the thyroid starts with the entry of mature CD3$^+$CD4$^+$ T cells followed by clustering of these cells with host DCs, expression of chemokines and adhesion molecules, and subsequent formation of PNAd$^+$ vessels.

A population of CD3$^-$CD4$^+$OX40L$^+$CD30$^+$ cells present in the adult spleen was recently described (41). Due to the phenotypical similarities with conventional neonatal LTi cells, these cells were named adult inducer cells (41), but to date there is no formal proof that these cells promote lymphoid organogenesis. We cannot fully rule out the possibility that such cells contribute to the formation of lymphoid aggregates described here, but they have been excluded in our highly purified preps, and we have been unable to document their presence in the thyroid prior to influx of CD3$^+$CD4$^+$ T cells. Furthermore, we have not detected differences in the expression of adhesion molecules or distribution of DCs prior to T cell transfer, which suggests that thyroids of noninjected RAGTGCCL21 mice are not primed for the formation of lymphoid structures. These results together with those obtained with the TGCCL21/Id2-deficient mice strongly suggest that the inducer cell in our model is a mature CD3$^+$CD4$^+$ T cell.

Entry of CD3$^+$CD4$^+$ T cells into the thyroid is determined by CCR7 expression. *CCR7*$^{-/-}$ cells do not enter thyroids of RAGTGCCL21 mice. Whether CCR7 expression is required for retention of T cells in the thyroid is unknown at this point. The current model for T cell trafficking into nonlymphoid tissue is that effector T cells enter the tissue as a function of the local production of inflammatory chemokines and that CCR7 expression is critical for reentry of T cells into lymphatics (42, 43). Our results indicate that CCR7-competent cells can reach the thyroid once CCL21 is ectopically expressed there, expanding the range of cells that can reach nonlymphoid tissue. Whether T cells are retained in the thyroid due to continued expression of CCR7 or to desensitization of CCR7 due to high tissue levels of CCL21 is unclear at this moment.

Entry of CD3$^+$CD4$^+$ T cells into thyroid induces clustering of DCs. The formation of the clusters is associated with increased expression of ICAM and VCAM in DCs and endothelial and stromal cells, expression of chemokines, and differentiation of endothelial cells. DC clusters form soon after T cells infiltrate the thyroid and are likely the consequence of DC influx rather than DC proliferation in situ. Several lines of evidence support an important role for CCR7 in DC trafficking. Migration of DCs into lymph nodes is severely impaired in the absence of CCR7 (30, 42, 43), and reduced lymphoid expression of CCR7 ligands CCL21 and CCL19 leads to reduced DC homing into lymph nodes (44). Our results, however, do not support a direct role for CCL21 in recruitment of DCs into the thyroid because thyroids of both RAG and RAGTGCCL21 mice have similar numbers of DCs prior to the injection of lymphocytes. Our results, however, support an indirect role for CCR7 signaling in the

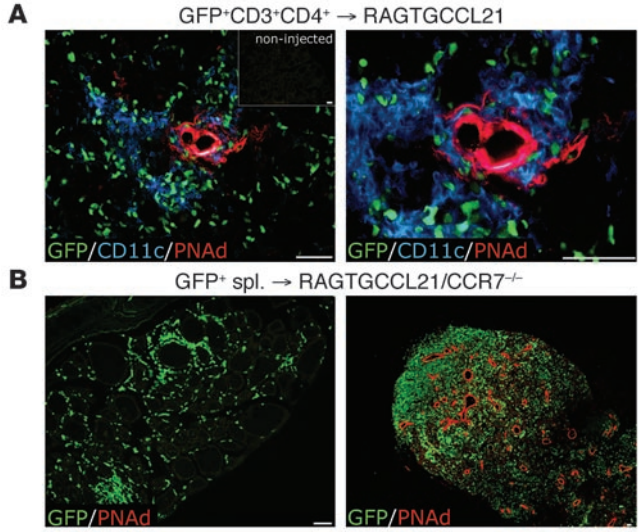


**Figure 7**
CD3+CD4+ T cells induce formation of PNAd+ vessels in thyroids of RAGTGCCL21 mice. (**A**) GFP+CD3+CD4+ T cells ($1 \times 10^6$) were injected i.v. into RAGTGCCL21 mice. Mice were sacrificed 10 days later, and thyroids were analyzed for the presence of GFP+ cells and PNAd+ vessels. PNAd+ vessels were not present in thyroids of RAGTGCCL21 mice prior to injection (inset) but were readily visualized (red) in thyroids of all mice injected with GFP+CD3+CD4+ T cells ($n > 50$ mice). In all cases, formation of PNAd+ structures was accompanied by the clustering of CD11c+ DCs (blue). (**B**) RAGTGCCL21/CCR7−/− mice were injected with $1 \times 10^7$ GFP+ splenocytes. One month after transfer, mice were sacrificed and thyroids analyzed for the presence of PNAd+ vessels. No PNAd+ vessels were observed in sections from *CCR7*-deficient recipients (>240 sections obtained from 8 mice). PNAd+ HEVs were readily detected in lymph nodes. Representative sections are presented. Scale bars: 0.05 mm.

influx and clustering of DCs because CCR7 deficiency affects the number and size of DC/T cell clusters in RAGTGCCL21/CCR7−/− recipients. Thus, our results suggest that CCL21 may activate incoming T cells to induce influx and clustering of DCs.

While CCR7 has an important role in migration of CD4+ T cells and DCs, its expression is clearly not sufficient for recruitment of B cells and CD8+ T cells. These cells also express CCR7 (45, 46) and thus would be expected to traffic into the thyroid as efficiently as CD3+CD4+ T cells, but they do not accumulate in the thyroid in the absence of CD3+CD4+ T cells. The lack of accumulation of these cell types could be due to the lack of additional signals or the lack of a favorable endothelial environment.

The influx of CD3+CD4+ T cells promoted marked changes in the expression of chemokines and adhesion molecules that are critical for further migration/retention of DCs, B cells, and T cells (33, 47, 48). For instance, marked changes were observed in the expression of the chemokine ligands CXCL9, CXCL10, CXCL11, CCL2, and CXCL16. CXCL9, CXCL10, and CXCL11 are ligands for CXCR3, which is expressed by T cells, DCs, and activated B cells (32, 33). CCL2, acting through its receptor CCR2, mobilizes DCs and T cells (47, 48). CXCL16 is expressed by myeloid DCs, and its receptor, CXCR6, is present in naive CD8+ T cells, NK T cells, and memory T cells (49, 50). Interestingly, production of CXCL9, CXCL10, CXCL11, and CCL2 by immune and follicular thyroid cells has been documented in the thyroids of patients with Hashimoto and Graves disease (51–54), highlighting an important role for these molecules in the pathogenesis of these conditions.

In addition, the development of specialized vascular structures may favor efficient cell trafficking into the thyroid. Here we demonstrate

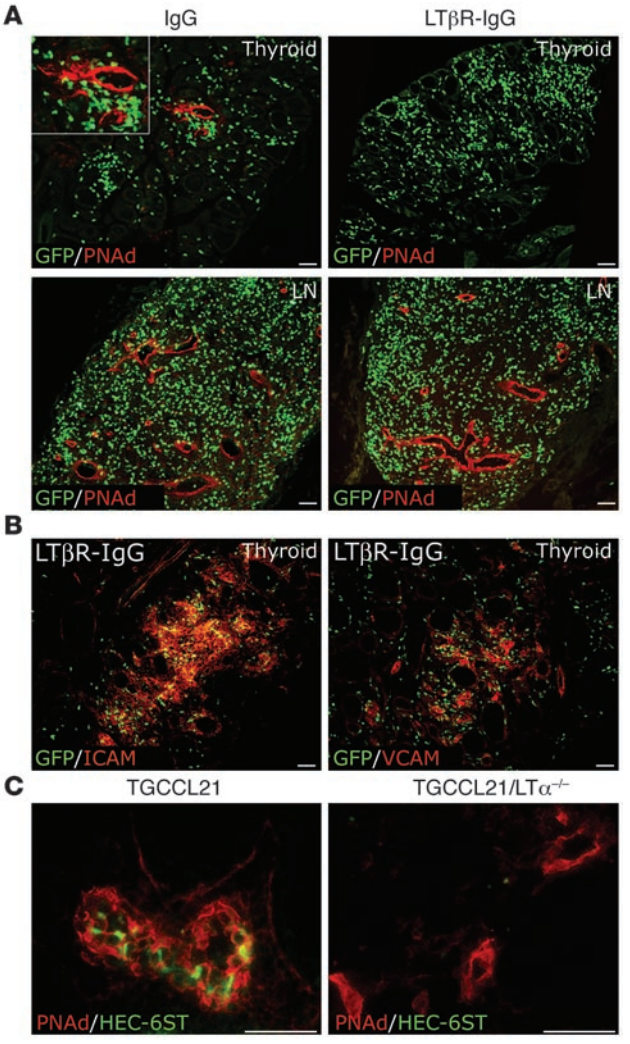


**Figure 8**
LTβR signaling regulates formation of PNAd+ structures in the thyroid. GFP+CD4+ T cells ($10^6$) were injected i.v. into RAGTGCCL21 mice. At days 1, 3, 5, and 7, mice were injected i.v. with 100 μg (400 μg total) of LTβR-IgG fusion protein. The control group was treated with mouse IgG. At day 10, mice were sacrificed and thyroids and lymph nodes analyzed for the presence of PNAd+ vessels. (**A**) PNAd+ vessels were readily detected in thyroids of all control mice ($n = 6$). In contrast, no PNAd+ cells were detected in thyroid sections (>800 sections from $n = 8$ mice) of animals treated with LTβR-IgG fusion protein. Inset shows a higher magnification (×40) of a PNAd+ vessel surrounded by GFP+ cells. (**B**) Expression of ICAM and VCAM was not affected by LTβR-IgG treatment. (**C**) PNAd+ vessels present in thyroids of TGCCL21 and TGCCL21/LTα−/− mice were analyzed for the expression of HEC-6ST, a marker of mature HEVs. PNAd+ vessels in thyroids of TGCCL21/LTα−/− mice had flat endothelia and did not express HEC-6ST, suggesting that they were not fully developed HEVs. Scale bars: 0.05 mm.

for what we believe is the first time that mature $CD3^+CD4^+$ T cells can induce formation of $PNAd^+$ vessels in nonlymphoid tissue. Induction of PNAd occurred as early as day 5 after T cell transfer; by day 10, $PNAd^+$ vessels were present in the thyroids of all mice examined. $PNAd^+$ vessels were always found in close proximity to the DC/T cell clusters. Interestingly, similar DC/T cell clusters have been observed in the synovial membranes of rheumatoid arthritis patients (55) and in colonic tissue of patients with Crohn disease (56). Thus, the differentiation of endothelial cells into $PNAd^+$ cells may be regulated by the interaction of T cells, DCs, and endothelial cells. DC/T cell clustering appears to be critical for these events because reduced clustering of DCs and T cells coincides with the impaired formation of $PNAd^+$ vessels. DC-derived signals affect the survival and homeostatic proliferation of T cells (57). These signals include soluble mediators as well as cell-surface molecules typically involved in T cell activation, such as MHC class II, CD80, CD86, and ICAM (57). We hypothesize that the reduced expression of PNAd associated with inefficient clustering of DCs and T cells may be due to the impaired differentiation or activation of T cells. Our results also highlight a role for CCR7 expressed by host cells in the formation of clusters and in the development of $PNAd^+$ vessels in the thyroid. However, our data do not limit the role of CCR7 to DCs and T cells, as CCR7 could regulate influx of other cell type(s) that may be involved in the induction of PNAd expression. As *CCR7* deficiency does not prevent formation of $PNAd^+$ HEVs in the lymph nodes or in the lungs (not shown), the formation of DC/T cell clusters and subsequent induction of $PNAd^+$ vessels may be regulated differently in distinct tissues.

Our results also indicate an important role for LTβR in the development of $PNAd^+$ vessels in nonlymphoid tissue. LTβR has a direct role in the maintenance of HEVs in the lymph nodes (19). While the LTβR-IgG dosing interval used in our study was not sufficient to disrupt PNAd expression in the lymph nodes, it prevented de novo formation of $PNAd^+$ vessels in the thyroid. LTβR is expressed by both DCs and endothelial cells within lymph nodes (58, 59). Expression of LTβR by thyroid endothelial cells could mediate expression of PNAd. As LTβR is also involved in the regulation of DC homeostasis (59), we cannot rule out that LTβR signaling at the level of DCs can also contribute to the development of $PNAd^+$ vessels. Which LTβR ligand mediates the induction of PNAd expression in the thyroid? To date, 2 ligands have been identified for LTβR: $LT\alpha1\beta2$ and LIGHT (reviewed in ref. 60). Residual flat $PNAd^+$ vessels that lack the expression of HEC-6ST are present within thyroids of LTα-deficient TGCCL21 mice, which lack both $LT\alpha3$ homotrimer and $LT\alpha1\beta2$ heterotrimer (24), suggesting an important role of $LT\alpha1\beta2$ for the maturation of HEVs. However, the interruption of LTβR signaling had a more pronounced effect, thus raising the possibility that LIGHT or another LTβR ligand not yet identified may contribute to the development of HEVs in the thyroid. The model described here can be used to answer this question and to study other aspects of HEV development in nonlymphoid tissue.

Although our chemokine-based model for the lymphocytic infiltration of the thyroid does not fully mimic human autoimmune thyroiditis, it does recapitulate the formation of organized lymphoid structures in the thyroid, which is the main histopathological feature in Hashimoto thyroiditis (61). Intriguingly, the importance of these structures for disease progression is still not understood. Lymphoid structures are frequently found in the thyroids of clinically asymptomatic middle-aged women and in the pancreas of NOD mice prior to the development of diabetes (reviewed in ref. 62), which suggests that they may actually play a role at an early stage of pathogenesis. Intriguingly, the formation of such lymphoid structures is favored during lymphopenic conditions. Our findings suggest that overexpression of chemokines (such as CCL21) due to viral or bacterial insults in nonlymphoid tissues (63–65) during lymphopenic conditions may initiate the formation of tertiary lymphoid tissue. Many reports link lymphopenia and autoimmune diseases, and lymphopenia is considered to be a factor contributing to autoimmunity induced by viral infections (reviewed in ref. 66). We observed that influx of $CD3^+CD4^+$ T cells in thyroids of RAGTGCCL21 mice coincided with the proliferation of these cells. We believe that the T cell proliferation observed in the thyroid is a function of homeostatic proliferation of T cells in a lymphopenic mouse, as we introduced lymphocytes into RAG-deficient mice. In agreement with this is the finding that, in fully developed lymphoid structures in thyroids of TGCCL21 mice, the proliferation rate of T cells decreases (Supplemental Figure 4), suggesting that once the lymphoid organ is formed, homeostatic mechanisms are activated to limit its size. Although we cannot fully exclude the possibility that proliferation of T cells in thyroids of RAGTGCCL21 mice involves additional antigenic stimulation, we do not have evidence to support such a hypothesis at present.

The models described here should contribute to a better understanding of the role of tertiary lymphoid structures in pathogenesis. Our findings suggest that formation of such structures may be promoted by expression of CCL21 and recruitment of $CD3^+CD4^+$ T cells. The presence of this T cell subset in the thyroid may be the nucleating event for development of the tertiary lymphoid structures that characterize this disease.

## Methods

*Mice*. Mice expressing *CCL21* under control of thyroglobulin promoter (TGCCL21) (24) were crossed to $RAG2^{-/-}$ mice (The Jackson Laboratory) to obtain a progeny that specifically expresses CCL21 in the thyroid and lacks T and B cells (RAGTGCCL21 mice). Genotyping of the TGCCL21-transgenic mice was conducted by PCR analysis as previously described (24). Mice with homozygous mutation of *RAG2* gene were identified by flow cytometry using anti-CD3 and anti-B220 antibodies (BD Biosciences — Pharmingen).

Transgenic mice expressing GFP (29) were backcrossed over 10 generations into the C57BL/6 background. Transgenic GFP mice were identified using a UV lamp. Mice obtained by crossing of GFP-transgenic mice with *CCR7*-deficient mice, described by Lipp and colleagues (30), are referred to as GFP/$CCR7^{-/-}$ mice. RAGTGCCL21 mice null for CCR7 are referred to as RAGTGCCL21/$CCR7^{-/-}$ mice. Mice conditionally expressing Flt3 ligand under a tetracycline-sensitive promoter have been previously described (31). Genotyping of the $Id2^{-/-}$ mice was performed by PCR using the following primers: 5′-CCTGGTGAAATGGCTGATAACAAAAGTC-3′; 5′-CTGAATTCCCTTCTGAGCTTATGTCG-3′; and 5′-CGCTCCCGATTCGCAGCGCATCGC-3′. *Id2*-deficient mice were crossed to TGCCL21 mice to obtain TGCCL21/$Id2^{-/-}$ mice. *LT*α-deficient mice were previously described (67). These mice were crossed with TGCCL21 mice to obtain TGCCL21/$LT\alpha^{-/-}$ mice.

All mice used for experiments were backcrossed at least 5 times into the C57BL/6 background. All mice were housed under specific pathogen–free conditions in individually ventilated cages at the Mount Sinai School of Medicine Animal Facility. All experiments were performed following institutional guidelines. Animal care and use of animals for experiments described in this study were approved by the Institutional Animal Care and Use Committee of Mount Sinai School of Medicine.

*Cell purification and transfer*. Single-cell suspensions were prepared by passing spleen tissue through a nylon mesh. Splenocytes ($1 \times 10^7$) were resuspended in 100 μl of PBS and injected into the retroorbital sinus. For the transfers of T and B cells, splenic single-cell suspensions were labeled using directly conjugated antibodies and sorted using a MoFlo High-Per-

formance Cell Sorter (Dako) according to standard protocols. Antibodies used were CD4 (RM4-5), CD3e (145-2C11), B220 (RA3-6B2), and CD8 (53–6.7) (BD Biosciences — Pharmingen). DC cells were sorted from the bone marrow of $GFP^+Flt3L^+$ mice treated with 3,000 ppm of doxycycline in the food for 7 days to increase the number of DCs. DCs were sorted using anti-CD11c (HL3) Abs (BD Biosciences — Pharmingen). The purity of the sorted populations was greater than 98%. To determine viability, samples were subsequently incubated with 20 μl of 5 μg/ml propidium iodide (Calbiochem) and analyzed using a FACSCanto flow cytometer (BD Biosciences — Pharmingen). For transfers, $1 \times 10^6$ purified cells were resuspended in 100 μl of PBS and injected into the retroorbital sinus. Mice were sacrificed at indicated time points, and thyroids and lymph nodes were removed and analyzed by immunohistochemistry.

*Histology*. Tissue samples were embedded in OCT buffer (Sakura) and snap frozen in 2-methylbutane (Merck) chilled in dry ice. Cryostat sections (8 μm) were fixed in acetone, blocked, and incubated with primary Abs in a humidified atmosphere for 1 hour at room temperature. After washing, conjugated secondary Abs were added and then incubated for 35 minutes. The slides were then washed and mounted with Fluoromount-G (SouthernBiotech). To preserve GFP signal, tissues from adaptively transferred animals were fixed in 1.6% paraformaldehyde (Electron Microscopy Science) containing 20% sucrose for 20 hours at 4°C. Analysis was performed using a Nikon fluorescence microscope. In some instances, images were overlayed and processed using Adobe Photoshop version 7.0. To improve visualization, we changed the original color obtained with Cy3 and Alexa Fluor 594 to blue (Figures 1, 4, and 6).

Primary antibodies used were specific for CD11c (HL3), CD3 (145-2C11), CD4 (L3T4), CD19 (1D3), CD45R/B220 (RA3-6B2), PNAd (MECA79), CD106 (VCAM-1) and CD54 (ICAM-1), CD35 (8C12) from BD Biosciences — Pharmingen, ER-TR7 from BMA Biomedicals, CXCL9 and CXCL16 from R&D Systems, and Ki67 from Novocastra. HEC-6ST antibody was previously described (39). Secondary antibodies used were Alexa Fluor 594 (emission wavelength 617 nm, red), goat anti-rat IgM, and goat anti-rat IgG; Alexa Fluor 488 (emission wavelength 519 nm, green), goat anti-rat IgG, and goat anti-rabbit IgG (Invitrogen); Cy3 (emission wavelength 570 nm, yellow), goat anti–Armenian hamster; and Cy5 (emission wavelength 670 nm, red), goat anti–Armenian hamster, and goat anti-rat (Jackson ImmunoResearch Laboratories Inc.).

*Analysis of mRNA expression*. Total RNA from thyroids was extracted using the RNeasy Mini Kit (QIAGEN) according to the manufacturer's instructions. Reverse transcription was performed using 2 μg of total RNA. Quantitative PCR was conducted in duplicates using 25 ng of reverse-transcribed cDNA and 0.4 μM of each primer in a 30-μl final reaction volume containing 1X SYBR Green PCR Master Mix (Applied Biosystems). PCR cycling conditions were as follows: 50°C for 2 minutes; 95°C for 10 minutes and 40 cycles of 95°C for 15 seconds; and 60°C for 1 minute. Relative expression levels were calculated as $2^{\text{threshold cycle [Ct] ubiquitin} - \text{Ct gene}}$ (for details see ABI PRISM 7700 Sequence Detection System, User Bulletin #2; http://hcgs.unh.edu/protocol/realtime/UserBulletin2.pdf) using Ubiquitin RNA as endogenous control. We used 2-tailed Student's *t* test to evaluate statistically significant differences in expression levels of specific chemokines. Primers were designed using Primer Express 2.0 software (Applied Biosystems). Primer sequences used are as follows: *CCL2*, forward GCTGGAGCATCCACGTGTT, reverse, ATCTTGCTGGTGAATGAGTAGCA; *CCL5*, forward, GCAAGTGCTCCAATCTTGCA, reverse, CTTCTCTGGGTTGGCACACA; *CCL8*, forward, GCTACGAGAGAATCAACAATATCCAGT, reverse, CAGAGAGACATACCCTGCTTGGT; *CXCL9*, forward, TGCACGATGCTCCTGCA, reverse, AGGTCTTTGAGGGATTTGTAGTGG; *CXCL10*, forward, GACGGTCCGCTGCAACTG, reverse, GCTTCCCTATGGCCCTCATT; *CXCL11*, forward, CGGGATGAAAGCCGTCAA, reverse, AACTTTGTCGCAGCCGTTACTC; *CXCL12*, forward, GCTCCTCGACAGATGCCTTG, reverse, GACCCTGGCACTGAACTGGA; *CXCL13*, forward, CATAGATCGGATTCAAGTTACGCC, reverse, TCTTGGTCCAGATCACAACTTCA; *CXCL16*, forward, AGCACACCAGCTTGGGTACC, reverse, CATGGCTGCAGTGAGGAAGA.

*LTβR blockade*. RAGTGCCL21 mice were treated with multiple doses of LTβR-IgG fusion protein (50 μg i.v.) as described (36, 37, 68). Treatment was done 1, 3, 5, and 7 days after transfer of $GFP^+CD4^+$ cells. Control mice received IgG only. On day 10, mice were sacrificed, and thyroids were removed and processed for immunofluorescence as described above.

*Statistics*. To evaluate statistical differences, we used unpaired 2-tailed Student's *t* tests. *P* values less than 0.05 were considered statistically significant.

## Acknowledgments

We thank Claudia Canasto-Chibuque for expert technical assistance. We are grateful to Jay Unkeless, Paul Frenette, Miriam Merad, and Antal Rot for critical comments on the manuscript and to Troy Randall, Martin Lipp, and Jonathon Sedgwick for providing us with the Id2, CCR7, and LTα mutant mice, respectively. This work was supported in part by a grant from the Irene Diamond Fund and by the NIH (DK 067989 to S.A. Lira and DK 57731 to N.H. Ruddle).

Received for publication May 4, 2006, and accepted in revised form August 1, 2006.

Address correspondence to: Sergio A. Lira, Immunobiology Center, Mount Sinai School of Medicine, 1425 Madison Avenue, Box 1630, New York, New York 10029-6574, USA. Phone: (212) 659-9404; Fax: (212) 849-2525; E-mail: sergio.lira@mssm.edu.

1. Mebius, R.E. 2003. Organogenesis of lymphoid tissues. *Nat. Rev. Immunol.* **3**:292–303.
2. Drayton, D.L., Liao, S., Mounzer, R.H., and Ruddle, N.H. 2006. Lymphoid organ development: from ontogeny to neogenesis. *Nat. Immunol.* **7**:344–353.
3. Eberl, G., and Littman, D.R. 2003. The role of the nuclear hormone receptor RORgammat in the development of lymph nodes and Peyer's patches. *Immunol. Rev.* **195**:81–90.
4. Yokota, Y., et al. 1999. Development of peripheral lymphoid organs and natural killer cells depends on the helix-loop-helix inhibitor Id2. *Nature.* **397**:702–706.
5. Kim, D., et al. 2000. Regulation of peripheral lymph node genesis by the tumor necrosis factor family member TRANCE. *J. Exp. Med.* **192**:1467–1478.
6. Muller, G., and Lipp, M. 2003. Concerted action of the chemokine and lymphotoxin system in secondary lymphoid-organ development. *Curr. Opin. Immunol.* **15**:217–224.
7. Futterer, A., Mink, K., Luz, A., Kosco-Vilbois, M.H., and Pfeffer, K. 1998. The lymphotoxin beta receptor controls organogenesis and affinity maturation in peripheral lymphoid tissues. *Immunity.* **9**:59–70.
8. Rennert, P.D., James, D., Mackay, F., Browning, J.L., and Hochman, P.S. 1998. Lymph node genesis is induced by signaling through the lymphotoxin beta receptor. *Immunity.* **9**:71–79.
9. De Togni, P., et al. 1994. Abnormal development of peripheral lymphoid organs in mice deficient in lymphotoxin. *Science.* **264**:703–707.
10. Koni, P.A., et al. 1997. Distinct roles in lymphoid organogenesis for lymphotoxins alpha and beta revealed in lymphotoxin beta-deficient mice. *Immunity.* **6**:491–500.
11. Soderberg, K.A., Linehan, M.M., Ruddle, N.H., and Iwasaki, A. 2004. MAdCAM-1 expressing sacral lymph node in the lymphotoxin beta-deficient mouse provides a site for immune generation following vaginal herpes simplex virus-2 infection. *J. Immunol.* **173**:1908–1913.
12. Rennert, P.D., Browning, J.L., and Hochman, P.S. 1997. Selective disruption of lymphotoxin ligands reveals a novel set of mucosal lymph nodes and unique effects on lymph node cellular organization. *Int. Immunol.* **9**:1627–1639.
13. Scheu, S., et al. 2002. Targeted disruption of LIGHT causes defects in costimulatory T cell activation and reveals cooperation with lymphotoxin beta in mesenteric lymph node genesis. *J. Exp. Med.* **195**:1613–1624.
14. Rot, A., and von Andrian, U.H. 2004. Chemokines in innate and adaptive host defense: basic chemokinese grammar for immune cells. *Annu. Rev. Immunol.*

**22**:891–928.
15. Miyasaka, M., and Tanaka, T. 2004. Lymphocyte trafficking across high endothelial venules: dogmas and enigmas. *Nat. Rev. Immunol.* **4**:360–370.
16. Drayton, D.L., et al. 2002. Lymphocyte traffic in lymphoid organ neogenesis: differential roles of Ltalpha and LTalphabeta. *Adv. Exp. Med. Biol.* **512**:43–48.
17. Ying, X., Chan, K., Shenoy, P., Hill, M., and Ruddle, N.H. 2005. Lymphotoxin plays a crucial role in the development and function of nasal-associated lymphoid tissue through regulation of chemokines and peripheral node addressin. *Am. J. Pathol.* **166**:135–146.
18. Drayton, D.L., Ying, X., Lee, J., Lesslauer, W., and Ruddle, N.H. 2003. Ectopic LT alpha beta directs lymphoid organ neogenesis with concomitant expression of peripheral node addressin and a HEV-restricted sulfotransferase. *J. Exp. Med.* **197**:1153–1163.
19. Browning, J.L., et al. 2005. Lymphotoxin-beta receptor signaling is required for the homeostatic control of HEV differentiation and function. *Immunity.* **23**:539–550.
20. Aloisi, F., and Pujol-Borrell, R. 2006. Lymphoid neogenesis in chronic inflammatory diseases. *Nat. Rev. Immunol.* **6**:205–217.
21. Cupedo, T., and Mebius, R.E. 2003. Role of chemokines in the development of secondary and tertiary lymphoid tissues. *Semin. Immunol.* **15**:243–248.
22. Fan, L., Reilly, C.R., Luo, Y., Dorf, M.E., and Lo, D. 2000. Cutting edge: ectopic expression of the chemokine TCA4/SLC is sufficient to trigger lymphoid neogenesis. *J. Immunol.* **164**:3955–3959.
23. Chen, S.C., et al. 2002. Ectopic expression of the murine chemokines CCL21a and CCL21b induces the formation of lymph node-like structures in pancreas, but not skin, of transgenic mice. *J. Immunol.* **168**:1001–1008.
24. Martin, A.P., et al. 2004. A novel model for lymphocytic infiltration of the thyroid gland generated by transgenic expression of the CC chemokine CCL21. *J. Immunol.* **173**:4791–4798.
25. Luther, S.A., Lopez, T., Bai, W., Hanahan, D., and Cyster, J.G. 2000. BLC expression in pancreatic islets causes B cell recruitment and lymphotoxin-dependent lymphoid neogenesis. *Immunity.* **12**:471–481.
26. Luther, S.A., et al. 2002. Differing activities of homeostatic chemokines CCL19, CCL21, and CXCL12 in lymphocyte and dendritic cell recruitment and lymphoid neogenesis. *J. Immunol.* **169**:424–433.
27. Cupedo, T., Jansen, W., Kraal, G., and Mebius, R.E. 2004. Induction of secondary and tertiary lymphoid structures in the skin. *Immunity.* **21**:655–667.
28. Fukuyama, S., et al. 2002. Initiation of NALT organogenesis is independent of the IL-7R, LTbetaR, and NIK signaling pathways but requires the Id2 gene and CD3(-)CD4(+)CD45(+) cells. *Immunity.* **17**:31–40.
29. Manfra, D.J., et al. 2001. Leukocytes expressing green fluorescent protein as novel reagents for adoptive cell transfer and bone marrow transplantation studies. *Am. J. Pathol.* **158**:41–47.
30. Forster, R., et al. 1999. CCR7 coordinates the primary immune response by establishing functional microenvironments in secondary lymphoid organs. *Cell.* **99**:23–33.
31. Manfra, D.J., et al. 2003. Conditional expression of murine Flt3 ligand leads to expansion of multiple dendritic cell subsets in peripheral blood and tissues of transgenic mice. *J. Immunol.* **170**:2843–2852.
32. Park, M.K., et al. 2002. The CXC chemokine murine monokine induced by IFN-gamma (CXC chemokine ligand 9) is made by APCs, targets lymphocytes including activated B cells, and supports antibody responses to a bacterial pathogen in vivo. *J. Immunol.* **169**:1433–1443.
33. Garcia-Lopez, M.A., et al. 2001. CXCR3 chemokine receptor distribution in normal and inflamed tissues: expression on activated lymphocytes, endothelial cells, and dendritic cells. *Lab. Invest.* **81**:409–418.
34. Bleul, C.C., Schultze, J.L., and Springer, T.A. 1998. B lymphocyte chemotaxis regulated in association with microanatomic localization, differentiation state, and B cell receptor engagement. *J. Exp. Med.* **187**:753–762.
35. MartIn-Fontecha, A., et al. 2003. Regulation of dendritic cell migration to the draining lymph node: impact on T lymphocyte traffic and priming. *J. Exp. Med.* **198**:615–621.
36. Wu, Q., et al. 1999. The requirement of membrane lymphotoxin for the presence of dendritic cells in lymphoid tissues. *J. Exp. Med.* **190**:629–638.
37. Browning, J.L., et al. 1997. Characterization of lymphotoxin-alpha beta complexes on the surface of mouse lymphocytes. *J. Immunol.* **159**:3288–3298.
38. Hemmerich, S., et al. 2001. Sulfation of L-selectin ligands by an HEV-restricted sulfotransferase regulates lymphocyte homing to lymph nodes. *Immunity.* **15**:237–247.
39. Bistrup, A., et al. 2004. Detection of a sulfotransferase (HEC-GlcNAc6ST) in high endothelial venules of lymph nodes and in high endothelial venule-like vessels within ectopic lymphoid aggregates: relationship to the MECA-79 epitope. *Am. J. Pathol.* **164**:1635–1644.
40. Armengol, M.P., et al. 2003. Chemokines determine local lymphoneogenesis and a reduction of circulating CXCR4+ T and CCR7 B and T lymphocytes in thyroid autoimmune diseases. *J. Immunol.* **170**:6320–6328.
41. Kim, M.Y., et al. 2003. CD4(+)CD3(-) accessory cells costimulate primed CD4 T cells through OX40 and CD30 at sites where T cells collaborate with B cells. *Immunity.* **18**:643–654.
42. Debes, G.F., et al. 2005. Chemokine receptor CCR7 required for T lymphocyte exit from peripheral tissues. *Nat. Immunol.* **6**:889–894.
43. Bromley, S.K., Thomas, S.Y., and Luster, A.D. 2005. Chemokine receptor CCR7 guides T cell exit from peripheral tissues and entry into afferent lymphatics. *Nat. Immunol.* **6**:895–901.
44. Gunn, M.D., et al. 1999. Mice lacking expression of secondary lymphoid organ chemokine have defects in lymphocyte homing and dendritic cell localization. *J. Exp. Med.* **189**:451–460.
45. Bjorkdahl, O., et al. 2003. Characterization of CC-chemokine receptor 7 expression on murine T cells in lymphoid tissues. *Immunology.* **110**:170–179.
46. Muller, G., Reiterer, P., Hopken, U.E., Golfier, S., and Lipp, M. 2003. Role of homeostatic chemokine and sphingosine-1-phosphate receptors in the organization of lymphoid tissue. *Ann. N. Y. Acad. Sci.* **987**:107–116.
47. Carr, M.W., Roth, S.J., Luther, E., Rose, S.S., and Springer, T.A. 1994. Monocyte chemoattractant protein 1 acts as a T-lymphocyte chemoattractant. *Proc. Natl. Acad. Sci. U. S. A.* **91**:3652–3656.
48. Osterholzer, J.J., et al. 2005. CCR2 and CCR6, but not endothelial selectins, mediate the accumulation of immature dendritic cells within the lungs of mice in response to particulate antigen. *J. Immunol.* **175**:874–883.
49. Tabata, S., et al. 2005. Distribution and kinetics of SR-PSOX/CXCL16 and CXCR6 expression on human dendritic cell subsets and CD4+ T cells. *J. Leukoc. Biol.* **77**:777–786.
50. Shimaoka, T., et al. 2003. Cutting edge: SR-PSOX/CXC chemokine ligand 16 mediates bacterial phagocytosis by APCs through its chemokine domain. *J. Immunol.* **171**:1647–1651.
51. Kemp, E.H., et al. 2003. Detection and localization of chemokine gene expression in autoimmune thyroid disease. *Clin. Endocrinol. (Oxf.).* **59**:207–213.
52. Rotondi, M., Lazzeri, E., Romagnani, P., and Serio, M. 2003. Role for interferon-gamma inducible chemokines in endocrine autoimmunity: an expanding field. *J. Endocrinol. Invest.* **26**:177–180.
53. Romagnani, P., et al. 2002. Expression of IP-10/CXCL10 and MIG/CXCL9 in the thyroid and increased levels of IP-10/CXCL10 in the serum of patients with recent-onset Graves' disease. *Am. J. Pathol.* **161**:195–206.
54. Garcia-Lopez, M.A., Sancho, D., Sanchez-Madrid, F., and Marazuela, M. 2001. Thyrocytes from autoimmune thyroid disorders produce the chemokines IP-10 and Mig and attract CXCR3+ lymphocytes. *J. Clin. Endocrinol. Metab.* **86**:5008–5016.
55. Van Dinther-Janssen, A.C., Pals, S.T., Scheper, R., Breedveld, F., and Meijer, C.J. 1990. Dendritic cells and high endothelial venules in the rheumatoid synovial membrane. *J. Rheumatol.* **17**:11–17.
56. Middel, P., Raddatz, D., Gunawan, B., Haller, F., and Radzun, H.J. 2005. Increased number of mature dendritic cells in Crohn's disease: evidence for a chemokine-mediated retention mechanism. *Gut.* **55**:220–227.
57. Feuillet, V., Lucas, B., Di Santo, J.P., Bismuth, G., and Trautmann, A. 2005. Multiple survival signals are delivered by dendritic cells to naive CD4(+) T cells. *Eur. J. Immunol.* **35**:2563–2572.
58. Drayton, D.L., et al. 2004. I kappa B kinase complex alpha kinase activity controls chemokine and high endothelial venule gene expression in lymph nodes and nasal-associated lymphoid tissue. *J. Immunol.* **173**:6161–6168.
59. Kabashima, K., et al. 2005. Intrinsic lymphotoxin-beta receptor requirement for homeostasis of lymphoid tissue dendritic cells. *Immunity.* **22**:439–450.
60. Ware, C.F. 2005. Network communications: lymphotoxins, LIGHT, and TNF. *Annu. Rev. Immunol.* **23**:787–819.
61. Weetman, A.P., and McGregor, A.M. 1994. Autoimmune thyroid disease: further developments in our understanding. *Endocr. Rev.* **15**:788–830.
62. Wicker, L.S., Todd, J.A., and Peterson, L.B. 1995. Genetic control of autoimmune diabetes in the NOD mouse. *Annu. Rev. Immunol.* **13**:179–200.
63. Humphreys, T.L., Baldridge, L.A., Billings, S.D., Campbell, J.J., and Spinola, S.M. 2005. Trafficking pathways and characterization of CD4 and CD8 cells recruited to the skin of humans experimentally infected with Haemophilus ducreyi. *Infect. Immun.* **73**:3896–3902.
64. Kurt, R.A., Brault, M.S., and Fried, B. 2003. Evidence of altered secondary lymphoid-tissue chemokine responsiveness in Balb/c mice infected with Schistosoma mansoni. *J. Parasitol.* **89**:721–725.
65. Bonacchi, A., et al. 2003. The chemokine CCL21 modulates lymphocyte recruitment and fibrosis in chronic hepatitis C. *Gastroenterology.* **125**:1060–1076.
66. Khoruts, A., and Fraser, J.M. 2005. A causal link between lymphopenia and autoimmunity. *Immunol. Lett.* **98**:23–31.
67. Korner, H., et al. 1997. Distinct roles for lymphotoxin-alpha and tumor necrosis factor in organogenesis and spatial organization of lymphoid tissue. *Eur. J. Immunol.* **27**:2600–2609.
68. Rennert, P.D., Browning, J.L., Mebius, R., Mackay, F., and Hochman, P.S. 1996. Surface lymphotoxin alpha/beta complex is required for the development of peripheral lymphoid organs. *J. Exp. Med.* **184**:1999–2006.